

The Role of Selective Transport in Neuronal Protein Sorting

Michelle A. Burack, Michael A. Silverman, and Gary Bunker*

Center for Research on Occupational and Environmental Toxicology
Oregon Health Sciences University
Portland, Oregon 97201

Summary

To assess whether selective microtubule-based vesicle transport underlies the polarized distribution of neuronal proteins, we expressed green fluorescent protein- (GFP-) tagged chimeras of representative axonal and dendritic membrane proteins in cultured hippocampal neurons and visualized the transport of carrier vesicles containing these proteins in living cells. Vesicles containing a dendritic protein, transferrin receptor (TfR), were preferentially transported into dendrites and excluded from axons. In contrast, vesicles containing the axonal protein NgCAM (neuron–glia cell adhesion molecule) were transported into both dendrites and axons. These data demonstrate that neurons utilize two distinct mechanisms for the targeting of polarized membrane proteins, one (for dendritic proteins) based on selective transport, the other (for axonal proteins) based on a selectivity “filter” that occurs downstream of transport.

Introduction

Neurons are compartmentalized into two molecularly and functionally distinct domains, axons and dendrites. The precise targeting and localization of proteins within these domains is critical for every aspect of neuronal function, from the localization of signaling molecules that govern axonal guidance to the distribution of channels that determine the integrative properties of dendrites (Goodman, 1996; Magee et al., 1998). Even the activity-dependent modification of synaptic strength that is thought to underlie neuronal plasticity may depend on the selective trafficking of neurotransmitter receptors (Frey and Morris, 1997; Malenka and Nicoll, 1999). Despite its fundamental importance, the mechanisms underlying neuronal protein targeting remain unclear, even for the most basic problem of sorting proteins differentially to axons or dendrites.

The targeting of proteins to different domains in polarized cells is thought to begin with the segregation of proteins into distinct populations of carrier vesicles (Craig and Bunker, 1994; Keller and Simons, 1997). Downstream of this event, little is known about the mechanisms which ensure that the sorted proteins reach only the correct membrane domain, for neurons or any other polarized cell type. There are two general possibilities (Goldstein and Yang, 2000): either the motor

proteins responsible for transporting the vesicles along microtubules to the plasma membrane are “smart”—i.e., they can distinguish between microtubules that lead to different destinations and transport the vesicles only to the correct domain—or the motors are “dumb,” and the selectivity occurs downstream of transport at the plasma membrane, e.g., via selective fusion or retention (Craig and Bunker, 1994; Foletti et al., 1999; Winckler and Mellman, 1999; Yeaman et al., 1999). In neurons, microtubule-based transport is required to move proteins the long distances from their site of synthesis in the soma to the plasma membrane of dendrites and axons; thus, a role for selective microtubule-based transport to direct sorted proteins into the correct domain has been widely posited (Black and Baas, 1989; Foletti et al., 1999; Stowell and Craig, 1999) but has never been directly demonstrated.

The development of green fluorescent protein (GFP) for following protein trafficking in living cells now makes it possible to assess the role of selective vesicle transport in protein sorting. We generated GFP-tagged chimeras of the dendritic protein transferrin receptor (TfR) and the axonal protein NgCAM (neuron–glia cell adhesion molecule) and monitored the transport of carrier vesicles containing these proteins in mature cultured hippocampal neurons. Our results show that selective microtubule-based transport does occur and is sufficient to account for the polarized distribution of TfR. We also show that NgCAM is transported into both dendrites and axons; thus, mechanisms downstream of transport are required to account for polarization of this protein at the axonal plasma membrane.

Results

GFP Chimeras Are Correctly Polarized at the Cell Surface

We chose two representative proteins whose polarized distributions in neurons are well characterized. TfR is a dendritic protein whose sorting depends on targeting sequences contained within its cytoplasmic domain (Cameron et al., 1991; West et al., 1997). Rat L1 is a cell adhesion molecule of the Ig superfamily that is highly polarized to axons (van den Pol and Kim, 1993; Winckler et al., 1999). Homologs of rat TfR and L1 from other species, which can be distinguished from the endogenous proteins using species-specific antibodies, are also appropriately polarized when expressed in hippocampal neurons using replication-defective viruses (Jareb and Bunker, 1998). We tagged human TfR and NgCAM (the avian homolog of L1) with GFP at their C termini and expressed the chimeric proteins in mature cultured hippocampal neurons using replication-defective herpesvirus. TfR is a type II membrane protein that places the C-terminal GFP tag in the luminal/extracellular domain. NgCAM is a type I membrane protein, which means that the C-terminal GFP tag is attached to NgCAM’s cytoplasmic domain.

To ensure that the virally expressed chimeras were

* To whom correspondence should be addressed (e-mail: bankerg@ohsu.edu).

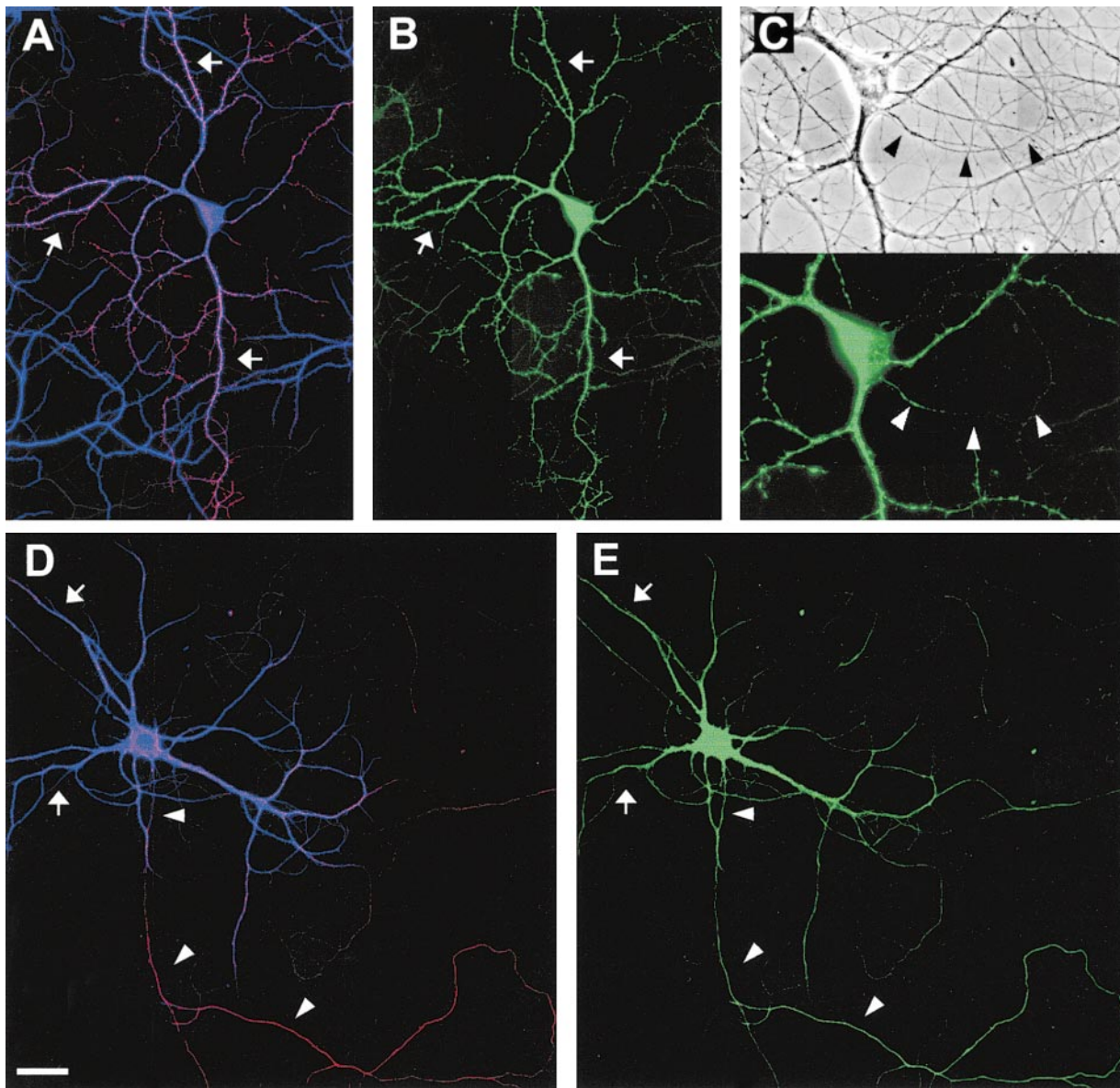


Figure 1. The Distribution of TfR-GFP and NgCAM-GFP Expressed in Mature Cultured Hippocampal Neurons with Replication-Defective Herpesvirus

Protein distribution was examined 24 hr after addition of virus.

(A) Cell surface TfR-GFP immunofluorescence (pseudocolored red) was highly polarized to dendrites (arrows), as illustrated by its colocalization with MAP2 immunofluorescence (pseudocolored blue; blue + red = magenta). The dendrites that are MAP2 positive and TFR negative arise from neighboring, uninfected cells.

(B and C) GFP fluorescence was polarized to the dendrites, indicating that intracellular TfR-GFP was excluded from all but the proximal axon (arrowheads in [C]).

(D) Cell surface NgCAM-GFP immunofluorescence (red) was polarized to the axon (arrowheads), indicated by the minimal colocalization with MAP2 (blue). The apparent cell surface staining of some distal dendrites actually arises from recurrent branches of the axon; dendrites that are not contacted by the axon lack cell surface staining (arrows).

(E) GFP fluorescence was uniformly distributed, indicating that dendrites contain significant amounts of intracellular NgCAM-GFP.

Scale bar, 10 μ m (A, B, D, and E); 20 μ m (C).

correctly sorted, we examined the cell surface distribution of the GFP-tagged proteins by incubating living cells with species-specific primary antibodies against the ectodomain of the expressed protein. As expected, cell surface TfR-GFP immunostaining was detected exclusively in dendrites (Figure 1A). Total TfR-GFP (cell surface and intracellular, represented by the GFP fluo-

rescence) was also restricted to dendrites (Figures 1B and 1C).

Cell surface immunostaining for NgCAM-GFP was also highly polarized (Figure 1D); like untagged NgCAM, the concentration of NgCAM-GFP on the axonal surface was 5- to 10-fold higher than on the dendritic surface (Jareb and Banker, 1998). Unexpectedly, intracellular

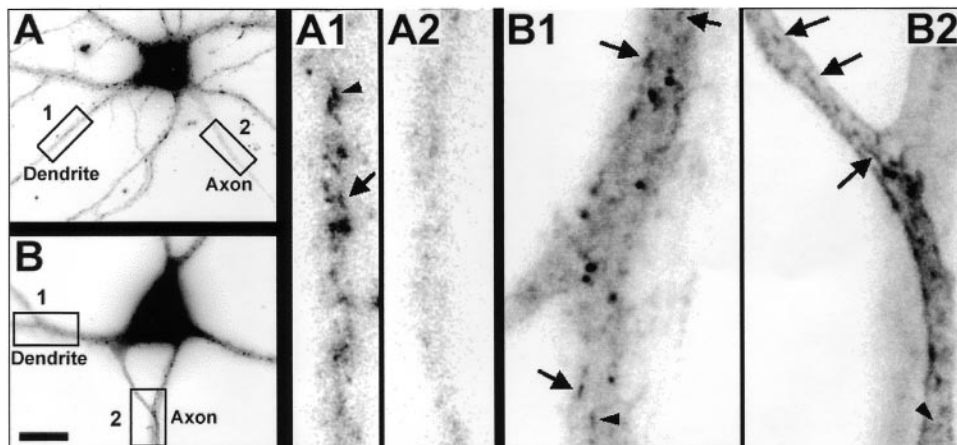


Figure 2. Localization of Transport Vesicles Containing GFP Chimeras in Living Neurons

For all panels, the contrast has been inverted so that fluorescent structures appear dark.

(A) TfR-GFP was associated with tubulovesicular organelles within dendrites. Examples of vesicles that moved anterogradely (arrow) or retrogradely (arrowhead) are indicated in the high magnification view of a single frame from a 30 s recording (A1). No moving TfR-GFP-labeled vesicles were detected in the axon (A2).

(B) NgCAM-GFP was present in mobile tubulovesicular organelles in both dendrites (B1) and the axon (B2). Examples of vesicles that moved anterogradely (arrows) or retrogradely (arrowheads) are indicated (see also Supplementary Video 1 [<http://www.neuron.org/cgi/content/full/26/2/465/DC1>]). The proximal axon runs along a neighboring dendrite, which lies in a different focal plane. The enhanced staining along the edge of the proximal axon reflects accumulation of NgCAM-GFP in the plasma membrane; this enhanced edge staining was not observed in dendrites.

Scale bar, 20 μm (left panels); 2.5 μm (right panels).

NgCAM-GFP was not polarized (Figure 1E). At 24 hr after infection, GFP fluorescence was present throughout the dendritic arbor, as well as in axons (Figure 1E). Untagged NgCAM detected by immunostaining in permeabilized cells was also abundant in dendrites, indicating that the GFP tag did not direct NgCAM to an inappropriate intracellular compartment (data not shown).

GFP Chimeras Label Mobile, Exocytic Vesicles

High magnification images of living neurons expressing TfR-GFP or NgCAM-GFP revealed that these proteins were associated with discrete tubulovesicular organelles (Figure 2). The organelles were highly pleiomorphic, ranging in shape from apparently spherical structures at or below the limit of resolution of light microscopy to tubular organelles more than a micrometer long. The variable morphology of these organelles is consistent with previous studies of transport carriers containing GFP-tagged plasma membrane proteins in other cell types (Hirschberg et al., 1998; Nakata et al., 1998; Toomre et al., 1999).

The pattern of NgCAM-GFP labeling at increasing times after the onset of expression was consistent with what would be expected for a protein that is transported in carrier vesicles and accumulates in the axonal plasma membrane. NgCAM-GFP fluorescence was first detectable in neuronal cell bodies 18–20 hr after virus addition. At this early time, we observed vesicular staining in the dendrites and axon; bright plasma membrane staining was limited to axonal growth cones, the site where NgCAM is preferentially added (Vogt et al., 1996). At progressively longer times after expression, membrane staining became more apparent throughout the axon (Figure 2B; see also Figure 5), eventually obscuring intracellular traffic.

In the case of TfR-GFP, accumulation of GFP fluorescence in the dendritic plasma membrane was not obvious. The staining pattern remained predominantly punctate even at late times after the onset of expression. This is not surprising, since TfR recycles rapidly between the plasma membrane and endosomes; at steady state, only a small fraction of the protein is present at the cell surface (Warren et al., 1997). To examine the relative proportions of GFP-labeled exocytic carrier vesicles versus endosomes, we incubated living neurons expressing TfR-GFP with primary antibody for 30 min before fixation. Bound antibody in endosomes was then detected by permeabilizing cells and incubating with labeled secondary antibodies. In proximal dendrites (10–20 μm from the soma), less than half of the vesicles were double labeled ($38.9\% \pm 4.4\%$, mean \pm SEM), indicating an abundance of putative exocytic carrier vesicles en route to the plasma membrane in this region (Figure 3). In more distal dendritic segments, double labeled organelles were more abundant ($54.7\% \pm 5.3\%$ at 50–60 μm from the soma), consistent with the expected rapid endocytosis of TfR from the dendritic plasma membrane (West et al., 1997). We therefore imaged vesicle transport at relatively early times after the onset of protein expression and focused our analysis on proximal dendrites to bias toward detecting the protein in exocytic vesicles.

To determine whether the GFP-labeled organelles had the expected transport properties of exocytic carrier vesicles, we performed time-lapse recordings from neurons expressing TfR-GFP or NgCAM-GFP. In these recordings, many of the vesicles moved at rates of 0.5–2.0 $\mu\text{m/s}$ (Figure 2; see also Supplementary Video 1 [<http://www.neuron.org/cgi/content/full/26/2/465/DC1>]), consistent with transport rates observed in earlier studies (Hirschberg et al., 1998; Nakata et al., 1998; Chao

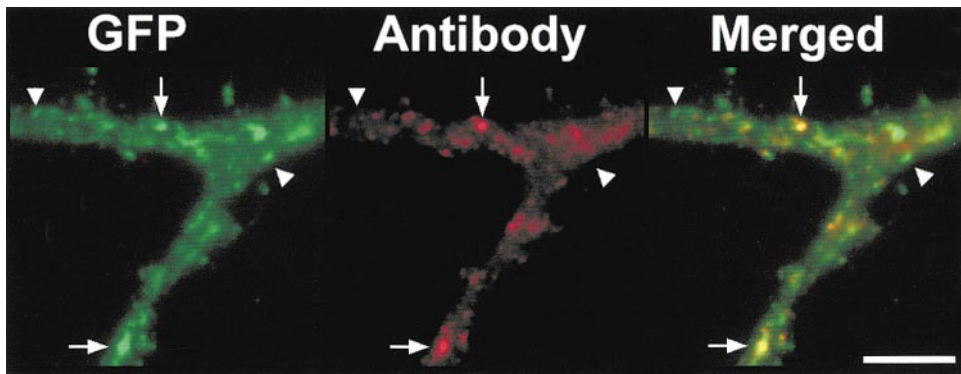


Figure 3. Antibody Uptake Experiments to Distinguish Endosomes from Exocytic Carrier Vesicles

Living neurons expressing TfR-GFP were incubated with primary antibody against TfR ectodomain for 30 min before fixation. Bound antibody present in endosomes was detected by permeabilizing cells, then incubating with labeled secondary antibodies. A segment of proximal dendrite is shown. Single labeled, antibody-negative structures (arrowheads), corresponding to exocytic vesicles, were common in this region of the cell. Double labeled structures, corresponding to endosomes, were also present (arrows). Scale bar, 5 μ m.

et al., 1999; Prekeris et al., 1999; Toomre et al., 1999). Transport of both constructs was bidirectional in dendrites; NgCAM-GFP vesicles also moved bidirectionally in axons, similar to previous observations of GFP-tagged plasma membrane proteins in axons of dorsal root ganglion neurons (Nakata et al., 1998). Transport was inhibited >80% following a 60–90 min incubation with the microtubule-disrupting agent, nocodazole, indicating that transport was microtubule based (TfR-GFP: $84.7\% \pm 8.5\%$ inhibition; NgCAM-GFP: $80.2\% \pm 9.6\%$, mean \pm SD).

Selectivity of Vesicle Transport

If protein polarization is determined by selective vesicle transport, then the number of vesicles containing a given protein that move from the cell body into axons or dendrites should reflect the degree of polarization of that protein at the cell surface. To assess this, we measured the number of anterogradely moving vesicles in the proximal dendrites and axons of cells expressing either TfR-GFP or NgCAM-GFP.

Transport of TfR-GFP was highly selective. Vesicles traveling away from the cell body were frequently observed within proximal dendrites but rarely entered the axon. This is illustrated by the cell shown in Figure 4. In a 30 s recording, 16 TfR-GFP vesicles were detected moving anterogradely within the proximal dendrite, but no anterogradely moving TfR-GFP vesicles were observed in the proximal axon (Figure 4; Supplementary Video 2 [<http://www.neuron.org/cgi/content/full/26/2/465/DC1>]). An analysis of eight cells confirmed that anterogradely moving TfR-GFP vesicles occurred far more frequently in dendrites than in axons (Table 1). No anterogradely moving TfR-GFP vesicles were observed in axons farther than 25 μ m from the cell body.

In contrast, vesicles containing the axonal membrane protein NgCAM-GFP were not selectively directed into the axon. In a representative cell, 22 NgCAM-GFP vesicles moved anterogradely in the proximal axon, and 15 NgCAM-GFP vesicles moved anterogradely in the proximal dendrite during a 30 s recording (Figure 5). Anterogradely moving NgCAM-GFP vesicles were observed throughout the dendritic arbor, even within distal

branches. Comparable results were obtained in all cells analyzed (Table 1).

Discussion

This report provides evidence that microtubule-based transport has the specificity required to target a sorted protein to the correct cellular domain. The transport of vesicles containing TfR was almost exclusively directed into dendrites, and this selective transport alone is sufficient to account for the polarization of TfR on the dendritic surface. Downstream selectivity mechanisms may also exist, but these would be redundant. Our results also show that selective transport is not required for the targeting of all polarized neuronal proteins. NgCAM is concentrated in the axonal plasma membrane despite its abundant transport into dendrites. Thus, our results demonstrate that at least two distinct mechanisms underlie the selective targeting of polarized proteins in nerve cells: one mechanism, for the targeting of dendritic proteins, operates at the level of microtubule-based transport; a second, for axonal proteins, operates at the level of the plasma membrane.

We cannot say whether these rules will hold for the targeting of all dendritic or axonal proteins. Presumably, the carrier vesicles, which were visualized by expressing GFP chimeras of representative dendritic or axonal proteins, also carry many other proteins destined for dendrites or for axons. It is not yet known how many distinct populations of carrier vesicles convey different proteins to axons or dendrites. For example, immunoisolation of organelles associated with different kinesins suggests that synaptic proteins may be transported into the axon in at least two distinct populations of carrier vesicles (Okada et al., 1995). In principle, the approach described here—based on imaging the transport of vesicles containing known proteins—can be used to determine the importance of selective transport for the targeting of any axonal or dendritic protein.

Our data indicate that the population of carrier vesicles that delivers the axonal protein NgCAM to the axon must be different from the population of vesicles that conveys the dendritic protein TfR to the dendrites. It has

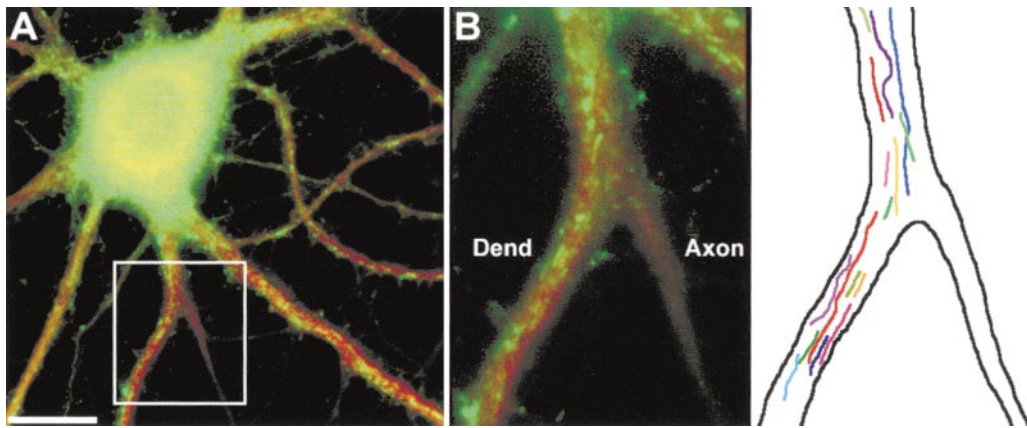


Figure 4. Selectivity of TfR-GFP Vesicle Transport

(A) Vesicle transport was recorded in the proximal dendrites and axon of a neuron (17 days in culture) expressing TfR-GFP. To confirm the identity of dendrites and the axon, the GFP image (pseudocolored green) was aligned with the MAP2 image (pseudocolored red) obtained after the neurons were fixed and immunostained at the end of the live cell recordings. In this neuron, the axon arose from a proximal dendrite, as indicated by the declining red MAP2 fluorescence in the right-hand branch of the dendrite in the box.

(B) Transport of TfR-GFP was highly selective. Vesicles containing TfR-GFP (green) were manually tracked from high magnification recordings of the proximal dendrite (Dend) and axon. The drawing shows the paths of all anterogradely moving vesicles observed in a 30 s recording; each vesicle path is indicated by a different colored line. Anterogradely moving vesicles were abundant in the proximal dendrite, but no vesicles entered the axon (see also Supplementary Video 2 [http://www.neuron.org/cgi/content/full/26/2/465/DC1]).

Scale bar, 15 μm (A); 5 μm (B).

always seemed likely that axonal and dendritic proteins travel in separate carriers, but it was also formally possible that the polarization of neuronal proteins depended solely on differences in their residence times in the dendritic and axonal plasma membrane. We do not know if the sorting of NgCAM and TfR into different carrier vesicles occurs at the *trans*-Golgi network or at a later sorting station, such as dendritic endosomes. However, if the vesicles that leave the *trans*-Golgi network contain both proteins, then nearly all of the axonal NgCAM must pass through the dendritic sorting compartment because TfR-containing vesicles almost never enter the axon.

The Basis for the Selective Transport of Dendritic Carrier Vesicles

Perhaps the most widely discussed model for the directed transport of neuronal proteins is that put forward 10 years ago by Black and Baas (1989) (see also Foletti

et al., 1999; Stowell and Craig, 1999; Goldstein and Yang, 2000). The model is based on the observation that dendrites have microtubules of mixed polarity orientation, whereas axonal microtubules have a uniform polarity orientation, with their plus ends toward the axon terminal (Baas et al., 1988). Black and Baas proposed that carrier vesicles containing dendritic proteins associate exclusively with minus end-directed motors, whereas vesicles carrying axonal proteins associate with plus end directed motors. If this were so, dendritic vesicles would be transported back and forth between soma and dendrites, but they would be excluded from axons because their minus end motors would drive them back toward the soma. Vesicles carrying axonal proteins would also travel bidirectionally between soma and dendrites, but in axons they would travel exclusively in the anterograde direction, leading to their eventual accumulation in the axonal domain.

Several observations suggest that this model, which assumes that each vesicle population associates with a single class of motor proteins, is oversimplified. First, carrier vesicles in the axon are capable of moving bidirectionally (this study; Nakata et al., 1998), indicating that they can associate with both plus and minus end-directed motors. In addition, although mature dendrites contain microtubules of mixed polarity orientation, the distal tips have uniformly plus end distal microtubules (Baas et al., 1988); thus, the transport of dendritic vesicles may also require both plus end and minus end-directed motors. Consistent with this idea, our preliminary observations indicate that TfR-containing vesicles are transported bidirectionally in immature dendrites (M. A. S. et al., unpublished data), which contain only plus end-distal microtubules (Baas et al., 1989).

How is it then that TfR vesicles translocate only along the subset of microtubules that enters dendrites? One possibility is that in mature neurons, dendritic vesicles

Table 1. Anterograde Transport of Vesicles Containing GFP Chimeras in the Proximal Axon and Dendrite

	Dendrite	Axon	Axon beyond 25 μm^a
(Vesicles/min)			
TfR-GFP	21.3 \pm 8.3	1.9 \pm 2.2	0
NgCAM-GFP	20.2 \pm 14.3	39.3 \pm 18.7	22.6 \pm 9.5

The number of anterogradely moving vesicles (mean \pm SD) in the proximal 50 μm of the axon and of one representative dendrite was measured for eight cells (17–28 days in culture). All vesicles with a minimum anterograde displacement of 1 μm (as measured from kymographs) were counted. Mean anterograde displacements were not significantly different for the two constructs and did not differ significantly between axons and dendrites.

^a The subset of anterogradely moving vesicles detected in the axonal segment beyond 25 μm from the cell body.

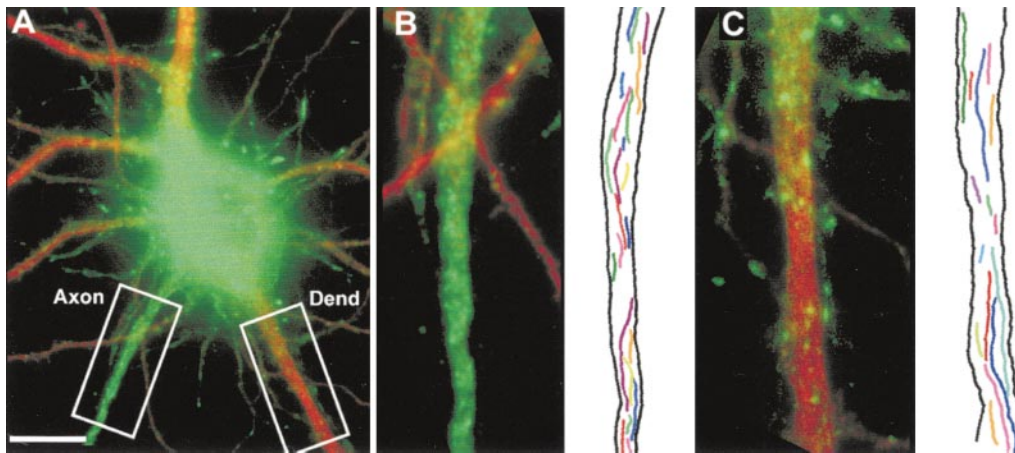


Figure 5. Transport of NgCAM-GFP Vesicles into Dendrites and the Axon

(A) Vesicle transport was recorded from the proximal axon and dendrites of a neuron (19 days in culture) expressing NgCAM-GFP. To confirm the identity of dendrites and the axon, the GFP image (pseudocolored green) was aligned with the MAP2 image (pseudocolored red) obtained after the neurons were fixed and immunostained at the end of live cell recordings. The intense GFP signal in the MAP2-negative axon reflects the combination of intracellular vesicles plus uniform cell surface staining (shown at higher magnification in [B]). MAP2-positive dendrites (Dend) have little cell surface NgCAM, but intracellular vesicles are apparent (shown at higher magnification in [C]).

(B and C) Transport of NgCAM-GFP was not selective. Vesicles containing NgCAM-GFP (green) were manually tracked from high magnification recordings of the proximal axon (B) and dendrite (C). The drawings illustrate the paths of all anterogradely moving vesicles observed in a 30 s recording; each vesicle path is indicated by a different colored line. Numerous anterogradely moving vesicles were observed in both the proximal axon and the proximal dendrite.

Scale bar, 15 μ m (A); 5 μ m (B and C).

utilize primarily minus end-directed motors, such as dynein or KIFC2 (Black and Baas, 1989; Hanlon et al., 1997; Saito et al., 1997), and plus end-directed motors are only utilized at early stages of development and in the distal dendrites of mature cells. Alternatively, dendritic vesicles may be transported out of the cell body by a smart plus end-directed motor that can distinguish between the microtubules that lead into dendrites and axons. Smart motors might translocate with different efficiencies on axonal and dendritic microtubules by recognizing differences in the biochemical properties of the microtubules, such as their association with different microtubule-associated proteins (Lopez and Sheetz, 1993, 1995; Craig and Bunker, 1994; Sato-Harada et al., 1996; Ebneth et al., 1998; Trinczek et al., 1999). Alternatively, the activity or cargo binding of smart motors might be differentially regulated in different cellular domains, e.g., by phosphorylation or dephosphorylation (McIlvain et al., 1994; Lee and Hollenbeck, 1995; Reilein et al., 1998). The plus end-directed motor KIF21B is enriched in dendrites, which suggests that it might translocate preferentially on dendritic microtubules (Marszalek et al., 1999). These properties make it a candidate for the kind of smart motor that could preferentially target TfR-containing vesicles into dendrites.

The Basis for the Axonal Targeting of NgCAM

The motor proteins that translocate axonal carrier vesicles labeled with NgCAM-GFP are dumb—they transport these vesicles into dendrites as well as axons. Thus, the axonal targeting of NgCAM must depend on selectivity mechanisms downstream of transport, most likely involving events at the plasma membrane. One possibility is that the NgCAM vesicles that enter dendrites are

unable to fuse with the dendritic plasma membrane; this would imply that the machinery that mediates constitutive exocytosis is different in axons and dendrites. The distributions of several molecular components of the exocytosis machinery, such as t-SNAREs and the sec6/sec8 complex, have been examined in neurons; to date, none has been reported to be polarized to axons or dendrites (Galli et al., 1995; Hazuka et al., 1999). Alternatively, NgCAM vesicles may fuse with the dendritic plasma membrane, but the protein is then rapidly redistributed to axons. Since a barrier at the axon hillock prevents proteins from diffusing from dendrites to axons within the membrane (Winckler et al., 1999), preferential removal of NgCAM from the dendritic membrane would require that its endocytosis (Kamiguchi et al., 1998) is differentially regulated in axons and dendrites.

Beyond Neuronal Polarity

The experiments in this paper focus on the role of selective, microtubule-based transport in the targeting of polarized proteins to axons or dendrites. The delivery of many important neuronal proteins must be regulated with far greater precision than this. Neurotransmitter receptors are an obvious example. Not only are receptors clustered at specific sites within dendrites, but their levels of expression on the cell surface appear to be controlled by synaptic activity (Nusser et al., 1998; Quinnian et al., 1999; Shi et al., 1999). Microtubule-based transport might also play a role in this “microtargeting” if it can be regulated by signaling events that are limited to discrete regions of the cell. If vesicle transport can be regulated by synaptic activity, this could promote the preferential delivery of receptors to “tagged” synapses within dendrites (Frey and Morris, 1998; Malenka and

Nicoll, 1999); if it can be regulated by pathfinding signals at the growth cone, it could allow preferential delivery of membrane constituents to axonal branches receiving an appropriate cue. The direct imaging of transport vesicles containing known GFP-tagged proteins in living cells can be used to examine these later events in the delivery of neuronal proteins, as well as the early events that are the topic of this report.

Experimental Procedures

DNA Constructs

GFP chimeras were generated in the plasmid vector pNF314 (Craig et al., 1995) and packaged into replication-defective herpesvirus (Ho, 1994). For both TfR and NgCAM, eGFP was added to the C terminus of the protein. pNF314-hTFR-eGFP was generated by PCR amplification of hTFR (pCDTR1; C. Enns, Oregon Health Sciences University) to change the stop codon to a Gly and introduce appropriate restriction sites for cloning in-frame with eGFP (Clontech). pNF314-NgCAM-eGFP was constructed by amplifying a 3', 350 bp fragment from pBS-NgCAM (P. Sonderregger, University of Zurich) to change the stop codon to a Leu and introduce appropriate restriction sites for cloning in-frame with eGFP. The resulting fragment was subcloned back into the original NgCAM vector, and the altered NgCAM cDNA was then subcloned into pNF314-eGFP. All PCR products were verified by sequencing.

Expression of Chimeric Proteins in Cultured Neurons

Primary hippocampal cultures were prepared from embryonic day 18 rat embryos, as previously described (Goslin et al., 1998). Neurons with mature dendritic arbors (14–28 days in culture) were used for all experiments. GFP chimeras were expressed using a defective herpesvirus (Geller and Breakefield, 1988) titrated to infect 1%–10% of neurons (see Jareb and Bunker, 1998). Vesicle transport was examined 20–28 hr after addition of virus. To detect proteins expressed on the cell surface, living cells were incubated with primary antibody diluted in culture medium for 5 min at 37°C, fixed, then permeabilized and processed for further immunostaining, as previously described (Jareb and Bunker, 1998).

Live Cell Imaging

Cultures were sealed into a heated chamber (Warner Instruments) in phenol red-free, riboflavin-free minimal essential medium supplemented with 30 μ M glucose, 1 mM pyruvate, 500 μ M kynurenic acid, 20 μ M trolox, and 60 μ M N-acetyl-cysteine. To examine inhibition of microtubule-based transport, 10 μ g/ml nocodazole was added to the recording medium in the chamber at the beginning of the experiment.

Neurons were imaged on a Leica DM-RXA microscope equipped with a 63 \times , 1.32 N. A. Plan Apo objective. Digital images were acquired with a Princeton Instruments Micromax CCD camera, capturing 600 ms exposures continuously for 20–60 s. A single level of focus was maintained throughout each recording. Recording at a single focal plane was usually sufficient to capture vesicle traffic throughout the full thickness of axons but not of proximal dendrites, which are significantly thicker. Thus, our measurements likely underestimated the amount of vesicle traffic in dendrites compared with axons. However, if the actual number of vesicles in dendrites is higher than we detected, this would only underscore the selectivity of transport for TfR and the lack of selectivity for NgCAM.

Neurons were fixed at the end of the recording and immunostained for MAP2 to confirm the identity of dendrites and axons. Digital images were processed and pseudocolored for presentation using MetaMorph imaging software (Universal Imaging) and Adobe Photoshop.

Analysis of Vesicle Transport

Vesicle transport was analyzed from the stored stacks of digital images using MetaMorph software. To most thoroughly account for all moving particles (as in Figures 4 and 5), the position of each vesicle was manually tracked using the track points function. For automated analysis of many cells (as in Table 1), the kymograph

function was used. This function generates a plot of the peak fluorescence intensity at each point along a neurite (displayed on the y axis) across time (displayed on the x axis). If the position of a fluorescent vesicle changes over time, it will give rise to a diagonal line on the kymograph; the slope of this line corresponds to the rate of vesicle movement. Although kymographs do not always display every moving vesicle, in our experience this method is as effective as manual tracking for providing an unbiased comparison of the relative number of transport events in axons and dendrites. In most cases, unprocessed stacks of digital images were used to generate the kymographs; however, for some cells the first image of the time series was subtracted from subsequent frames to remove stationary fluorescence and enhance detection of moving particles.

For analysis of nocodazole inhibition, transport at baseline (10–20 min after addition of nocodazole, the earliest time at which recordings could be initiated) was compared with transport in the same cells after 60–90 min in nocodazole. Since both anterograde and retrograde movements were inhibited, the data for transport in each direction were pooled for the analysis. Total transport was computed by summing the net translocations of all vesicles (absolute value of Δ -Y measured from kymographs) in a 12 s recording. The percent inhibition was calculated as total transport after 60–90 min in nocodazole \div total transport at baseline ($n = 3$ cells for TfR, $n = 4$ cells for NgCAM). For NgCAM, axons and dendrites were affected similarly, and the data were pooled for the analysis.

Analysis of GFP and Antibody Colocalization

Living neurons expressing TfR-GFP (20 hr after addition of virus) were incubated with primary antibody against the ectodomain of TfR (B3/25, Boehringer Mannheim) for 30 min prior to fixation and permeabilization. Primary antibody was detected using Cy3-labeled secondary antibodies. Digital images of GFP and immunofluorescence signals were acquired using a 63 \times objective. Proximal and distal segments (10–20 μ m and 50–60 μ m from the soma, respectively, $n = 7$ each) were selected from five neurons for analysis. TfR-GFP-containing vesicles were traced individually on the GFP image; these tracings were then overlaid on the immunofluorescence image, and tracings that contained bright immunofluorescence were scored as double labeled.

Acknowledgments

We thank J. Muyskens for the preparation of neuronal cultures; N. Glicksman for assistance with motion analysis; and A. M. Craig, C. Enns, A. Futterman, S. Green, M. Jareb, S. Kaech, and B. Sampo for their comments on the manuscript. This work was supported by National Institutes of Health grant NS17112.

Received January 28, 2000; revised March 10, 2000.

References

- Baas, P.W., Deitch, J.S., Black, M.M., and Bunker, G.A. (1988). Polarity orientation of microtubules in hippocampal neurons: uniformity in the axon and nonuniformity in the dendrite. *Proc. Natl. Acad. Sci. USA* **85**, 8335–8339.
- Baas, P.W., Black, M.M., and Bunker, G.A. (1989). Changes in microtubule polarity orientation during the development of hippocampal neurons in culture. *J. Cell Biol.* **109**, 3085–3094.
- Black, M.M., and Baas, P.W. (1989). The basis of polarity in neurons. *Trends Neurosci.* **12**, 211–214.
- Cameron, P.L., Sudhof, T.C., Jahn, R., and De Camilli, P. (1991). Colocalization of synaptophysin with transferrin receptors: implications for synaptic vesicle biogenesis. *J. Cell Biol.* **115**, 151–164.
- Chao, D.S., Hay, J.C., Winnick, S., Prekeris, R., Klumperman, J., and Scheller, R.H. (1999). SNARE membrane trafficking dynamics in vivo. *J. Cell Biol.* **144**, 869–881.
- Craig, A.M., and Bunker, G. (1994). Neuronal polarity. *Annu. Rev. Neurosci.* **17**, 267–310.
- Craig, A.M., Wyborski, R.J., and Bunker, G. (1995). Preferential addition of newly synthesized membrane protein at axonal growth cones. *Nature* **375**, 592–594.

Ebneth, A., Godemann, R., Stamer, K., Illenberger, S., Trinczek, B., and Mandelkow, E. (1998). Overexpression of tau protein inhibits kinesin-dependent trafficking of vesicles, mitochondria, and endoplasmic reticulum: implications for Alzheimer's disease. *J. Cell Biol.* **143**, 777–794.

Foletti, D.L., Prekeris, R., and Scheller, R.H. (1999). Generation and maintenance of neuronal polarity: mechanisms of transport and targeting. *Neuron* **23**, 641–644.

Frey, U., and Morris, R.G. (1998). Synaptic tagging: implications for late maintenance of hippocampal long-term potentiation. *Trends Neurosci.* **21**, 181–188.

Frey, U., and Morris, R.G.M. (1997). Synaptic tagging and long-term potentiation. *Nature* **385**, 533–536.

Galli, T., Garcia, E.P., Mundigl, O., Chilcote, T.J., and De Camilli, P. (1995). v- and t-SNAREs in neuronal exocytosis: a need for additional components to define sites of release. *Neuropharmacology* **34**, 1351–1360.

Geller, A.I., and Breakefield, X.O. (1988). A defective HSV-1 vector expresses Escherichia coli beta-galactosidase in cultured peripheral neurons. *Science* **241**, 1667–1669.

Goldstein, L.S.B., and Yang, Z. (2000). Microtubule-based transport systems in neurons: the roles of kinesins and dyneins. *Annu. Rev. Neurosci.* **23**, 39–72.

Goodman, C.S. (1996). Mechanisms and molecules that control growth cone guidance. *Annu. Rev. Neurosci.* **19**, 341–377.

Goslin, K., Asmussen, H., and Banker, G. (1998). Rat hippocampal neurons in low-density culture. In *Culturing Nerve Cells*, G. Banker and K. Goslin, eds. (Cambridge, MA: MIT Press), pp. 339–370.

Hanlon, D.W., Yang, Z., and Goldstein, L.S. (1997). Characterization of KIFC2, a neuronal kinesin superfamily member in mouse. *Neuron* **18**, 439–451.

Hazuka, C.D., Foletti, D.L., Hsu, S.C., Kee, Y., Hopf, F.W., and Scheller, R.H. (1999). The sec6/8 complex is located at neurite outgrowth and axonal synapse-assembly domains. *J. Neurosci.* **19**, 1324–1334.

Hirschberg, K., Miller, C.M., Ellenberg, J., Presley, J.F., Siggia, E.D., Phair, R.D., and Lippincott-Schwartz, J. (1998). Kinetic analysis of secretory protein traffic and characterization of golgi to plasma membrane transport intermediates in living cells. *J. Cell Biol.* **143**, 1485–1503.

Ho, D.Y. (1994). Amplicon-based herpes simplex virus vectors. *Methods Cell Biol.* **43**, 191–210.

Jareb, M., and Banker, G. (1998). The polarized sorting of membrane proteins expressed in cultured hippocampal neurons using viral vectors. *Neuron* **20**, 855–867.

Kamiguchi, H., Long, K.E., Pendergast, M., Schaefer, A.W., Rapoport, J., Kirchhausen, T., and Lemmon, V. (1998). The neural cell adhesion molecule L1 interacts with the AP-2 adaptor and is endocytosed via the clathrin-mediated pathway. *J. Neurosci.* **18**, 5311–5321.

Keller, P., and Simons, K. (1997). Post-Golgi biosynthetic trafficking. *J. Cell Sci.* **110**, 3001–3009.

Lee, K.D., and Hollenbeck, P.J. (1995). Phosphorylation of kinesin in vivo correlates with organelle association and neurite outgrowth. *J. Biol. Chem.* **270**, 5600–5605.

Lopez, L.A., and Sheetz, M.P. (1993). Steric inhibition of cytoplasmic dynein and kinesin motility by MAP2. *Cell Motil. Cytoskel.* **24**, 1–16.

Lopez, L.A., and Sheetz, M.P. (1995). A microtubule-associated protein (MAP2) kinase restores microtubule motility in embryonic brain. *J. Biol. Chem.* **270**, 12511–12517.

Magee, J., Hoffman, D., Colbert, C., and Johnston, D. (1998). Electrical and calcium signaling in dendrites of hippocampal pyramidal neurons. *Annu. Rev. Physiol.* **60**, 327–346.

Malenka, R.C., and Nicoll, R.A. (1999). Long-term potentiation—a decade of progress? *Science* **285**, 1870–1874.

Marszalek, J.R., Weiner, J.A., Farlow, S.J., Chun, J., and Goldstein, L.S. (1999). Novel dendritic kinesin sorting identified by different process targeting of two related kinesins: KIF21A and KIF21B. *J. Cell Biol.* **145**, 469–479.

McIlvain, J.M., Burkhardt, J.K., Hamm-Alvarez, S., Argon, Y., and Sheetz, M.P. (1994). Regulation of kinesin activity by phosphorylation of kinesin-associated proteins. *J. Biol. Chem.* **269**, 19176–19182.

Nakata, T., Terada, S., and Hirokawa, N. (1998). Visualization of the dynamics of synaptic vesicle and plasma membrane proteins in living axons. *J. Cell Biol.* **140**, 659–674.

Nusser, Z., Hajos, N., Somogyi, P., and Mody, I. (1998). Increased number of synaptic GABA(A) receptors underlies potentiation at hippocampal inhibitory synapses. *Nature* **395**, 172–177.

Okada, Y., Yamazaki, H., Sekine-Aizawa, Y., and Hirokawa, N. (1995). The neuron-specific kinesin superfamily protein KIF1A is a unique monomeric motor for anterograde axonal transport of synaptic vesicle precursors. *Cell* **81**, 769–780.

Prekeris, R., Foletti, D.L., and Scheller, R.H. (1999). Dynamics of tubulovesicular recycling endosomes in hippocampal neurons. *J. Neurosci.* **19**, 10324–10337.

Quinlan, E.M., Philpot, B.D., Huganir, R.L., and Bear, M.F. (1999). Rapid, experience-dependent expression of synaptic NMDA receptors in visual cortex in vivo. *Nat. Neurosci.* **2**, 352–357.

Reilein, A.R., Tint, I.S., Peunova, N.I., Enikolopov, G.N., and Gelfand, V.I. (1998). Regulation of organelle movement in melanophores by protein kinase A (PKA), protein kinase C (PKC), and protein phosphatase 2A (PP2A). *J. Cell Biol.* **142**, 803–813.

Saito, N., Okada, Y., Noda, Y., Kinoshita, Y., Kondo, S., and Hirokawa, N. (1997). KIFC2 is a novel neuron-specific C-terminal type kinesin superfamily motor for dendritic transport of multivesicular body-like organelles. *Neuron* **18**, 425–438.

Sato-Harada, R., Okabe, S., Umeyama, T., Kanai, Y., and Hirokawa, N. (1996). Microtubule-associated proteins regulate microtubule function as the track for intracellular membrane organelle transports. *Cell Struct. Funct.* **21**, 283–295.

Shi, S.H., Hayashi, Y., Petralia, R.S., Zaman, S.H., Wenthold, R.J., Svoboda, K., and Malinow, R. (1999). Rapid spine delivery and redistribution of AMPA receptors after synaptic NMDA receptor activation. *Science* **284**, 1811–1816.

Stowell, J.N., and Craig, A.M. (1999). Axon/dendrite targeting of metabotropic glutamate receptors by their cytoplasmic carboxy-terminal domains. *Neuron* **22**, 525–536.

Toomre, D., Keller, P., White, J., Olivo, J.C., and Simons, K. (1999). Dual-color visualization of trans-Golgi network to plasma membrane traffic along microtubules in living cells. *J. Cell Sci.* **112**, 21–33.

Trinczek, B., Ebneth, A., Mandelkow, E.M., and Mandelkow, E. (1999). Tau regulates the attachment/detachment but not the speed of motors in microtubule-dependent transport of single vesicles and organelles. *J. Cell Sci.* **112**, 2355–2367.

van den Pol, A.N., and Kim, W.T. (1993). NILE/L1 and NCAM-polysialic acid expression on growing axons of isolated neurons. *J. Comp. Neurol.* **332**, 237–257.

Vogt, L., Giger, R.J., Ziegler, U., Kunz, B., Buchstaller, A., Hermens, W.T.J.M.C., Kaplitt, M.G., Rosenfeld, M.R., Pfaff, D.W., Verhaagen, J., and Sonderegger, P. (1996). Continuous renewal of the axonal pathway sensor apparatus by insertion of new sensor molecules into the growth cone membrane. *Curr. Biol.* **6**, 1153–1158.

Warren, R.A., Green, F.A., and Enns, C.A. (1997). Saturation of the endocytic pathway for the transferrin receptor does not affect the endocytosis of the epidermal growth factor receptor. *J. Biol. Chem.* **272**, 2116–2121.

West, A.E., Neve, R.L., and Buckley, K.M. (1997). Identification of a somatodendritic targeting signal in the cytoplasmic domain of the transferrin receptor. *J. Neurosci.* **17**, 6038–6047.

Winckler, B., and Mellman, I. (1999). Neuronal polarity: controlling the sorting and diffusion of membrane components. *Neuron* **23**, 637–640.

Winckler, B., Forscher, P., and Mellman, I. (1999). A diffusion barrier maintains distribution of membrane proteins in polarized neurons. *Nature* **397**, 698–701.

Yeaman, C., Grindstaff, K.K., and Nelson, W.J. (1999). New perspectives on mechanisms involved in generating epithelial cell polarity. *Physiol. Rev.* **79**, 73–98.